doi:10.3233/STAL190165

Behavior of a Geosynthetic-Reinforced Soil Retaining Wall Under Seismic Loading

Cecilia TORRES QUIROZ[a,1], Marko LÓPEZ BENDEZÚ[b], Jorge ZEGARRA PELLANNE[b] and Celso ROMANEL[c]
[a]*Departamento Académico de Ingeniería Geotécnica, Universidad Nacional de Ingeniería (UNI), Peru*
[b]*Departamento de Ingeniería, Sección de Ingeniería Civil, Pontificia Universidad Católica del Perú (PUCP), Peru*
[c]*Departamento de Engenharia Civil e Ambiental, Pontificia Universidade Católica do Rio de Janeiro (PUC-Rio), Brasil*

Abstract. Geosynthetic- reinforced soil (GRS) walls have become a good alternative in the Peruvian seismic areas due to their flexible nature and cost effectiveness over conventional retaining structures. In the practice of engineering, the analysis and design of GRS are done through limit-equilibrium methods, under static conditions, or using pseudo static methods when earthquake loads are involved. In this paper, a numerical analysis investigates the dynamic behavior of a geosynthetic reinforced soil retaining wall in Arequipa – Peru due to earthquake loading. The assumptions and methods for both the static and dynamic analysis will be fully described, from the conceptual model, choice of soil parameters and reinforcement to discussion of results. This procedure considered both the foundation soil deformability and seismic amplification of the soil. The earthquakes were generated by adjusting the history acceleration of local earthquakes to the obtained design acceleration spectrum through the seismic hazard study for a specific site. Main conclusions of the results to current pseudo-static seismic design methods and numerical analysis for reinforced soil walls turn around the failure zone, contributions of the reinforcement element and the global behavior of the structure, which are discussed in this paper.

Keywords. numerical simulation, geosynthetic-reinforced soil retaining wall, earthquake response, finite difference method.

1. Introduction

The Geosynthetic Reinforced Soil (GRS) walls are geotechnical structures used in the stabilization of embankments. The construction of this structure consists of the compaction of the filling material together with a reinforcement element to form at the end a soil-reinforcement system structure with greater shear strength, allowing ~~that~~ the construction of greater heights structures to be reached with less inclined angles.

What defines a GRS wall is the type of reinforcement, which depends on its rigidity, the tensile strength and its ability to deform. In this context AASHTO (American Association of State Highway and Transportation Officials) classifies the reinforcements,

[1] Departamento Académico de Ingeniería Geotécnica, Universidad Nacional de Ingeniería, Peru; E-mail: ctorresq@uni.pe.

according to the material and extensibility, as inextensible (steel) or extensible (geosynthetics).

The inclusion of an element with tensile strength between soil layers allows the soil-reinforcement system to improve its performance with respect to shearing failure. This happens basically due to the friction forces developed in the soil-reinforcement contact. GRS wall structures have shown good performance in cases of earthquakes, as described by several authors considering the behavior of real or reduced scale models.

Burke et al. [1] made the comparison between the seismic response of a reinforced soil wall and the results predicted by a finite element analysis, concluding that the numerical model was able to correctly simulate the dynamic behavior of the structure. Pamuk et al. [2] also found a good correlation between observed and predicted displacements in a reinforced soil wall subjected to accelerations generated by the Kokaelly earthquake, occurred in Turkey in 1999.

In the engineering practice, numerical analysis is not often considered for this type of structure, due to the extensive information required to represent the dynamic behavior of reinforced walls but, on the other hand, results determined using conventional methodologies can be very conservative.

In this article, for the design of geosynthetic reinforced soil (GRS) walls, the computer program MSEW v3.0 was used, which allows to evaluate the internal and external stability of the structure. The static and pseudo static global stability analyses were carried out with Slide v6.0 program while the seismic behavior was evaluated with FLAC 2D v.7.0.

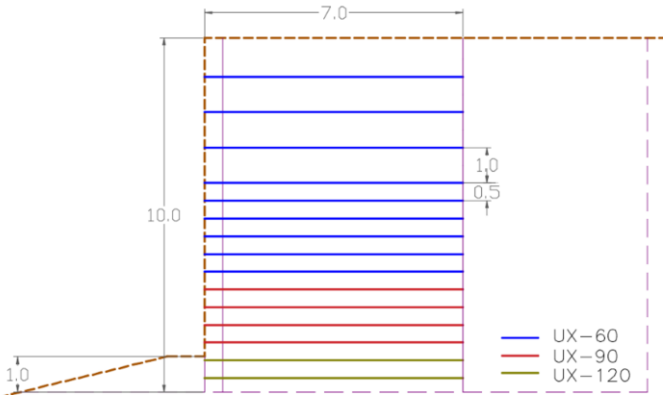

Figure 1. Schematic of GRS wall design with unequal spacing and uniform length, also this scheme matched with the final reinforcement configuration of the structure GRS.

2. Standard regulations

The GRS wall was designed with uniaxial geogrids as reinforcements. This kind of wall was selected for the present study because under seismic condition it allows to withstand large deformations without losing its service condition. The reinforcement presents unequal spacing and uniform length [3], which allows optimizing the amounts of reinforcement to be used. In addition, the following design considerations were taken:

- The GRS wall will be formed from 1 m below the natural terrain. The AASTHO standard recommends 0.6 m or one-tenth of the height as a minimum.

- Flat surface on the top of the structure for projected temporal facilities.
- According to recommendations of FHWA [4] and AASTHO the minimum reinforcement length is 0.7 times the height of the wall ($L_{min} \geq 0.7$ H), where H is the total height of the wall. It is also indicated that for seismic analysis this length could be greater, with recommendation that $L_{min} = 0.8$ H.
- Infiltration or phreatic level problems were discharged under the statement that this structure will be built with a drainage system.

Figure 1 shows the layout of the GRS wall, where the spacing between layers is every 0.5 m and 1 m and each color represents a kind of reinforcement.

3. Site conditions

The construction site of the GRS wall is situated in Tambomayo at an altitude of 4850 msnm, in the province of Castilla in Arequipa, southern Peru. The area has an irregular surface with steep slope changes and presents rocky outcrops of volcanic origin corresponding to the Orcopampa formation and andesitic flows of the Mismi volcanic complex of the Barroso Group. It was found, from perforations made during the geotechnical investigation, which the rock below 15m varies between an andesitic tuff and an andesite.

The climate is cold with high relative humidity in the winter months accompanied by intense snowfall and presence of fog; in summer, there are sunny days and freezing nights. The scant vegetation is restricted to some cacti and parasitic plants, typical of the Puna desert areas. The water from rains flows through the Tambomayo creek and other tributaries, through the drainage and sub-drainage systems associated with the project. Due to this reason, the influence of the water within the analyses will not be taken into account.

The selection of the seismic coefficient was according with the FHWA [5] standard which recommends that the seismic coefficient be 50% of the maximum horizontal acceleration in terms of g (gravity acceleration). The study of seismic hazard determined that the maximum acceleration for a return time of 475 years is 0.38g; therefore, the value considered for pseudo static analyses is 0.19g [6].

4. Parameters for design

The characterization of five components has been established: the foundation soil, the reinforced soil, the retained soil, material for the facade (stones placed in baskets), and the reinforcing elements (uniaxial geogrids). The geotechnical investigation program carried out in the Tambomayo site in 2013 allowed to characterize the materials. Table 1 presents the geotechnical parameters adopted for the design of the GSW by internal and external stability analysis considering a wall of 10m maximum height.

Table 2 shows the physical and mechanical properties of the high strength polyester fiber coated with long-lasting polymer used as reinforcement for the design of the reinforced wall.

The main nominal external load acting on the wall is the ground pressure exerted by the soil retained behind it and some overloads above the reinforced soil. For the case evaluated in the present investigation, the effect of ground pressures on the 10m wall is

much greater than the effect of the overloads (which could simulate a live load of vehicle traffic or light temporary structures). Therefore, to simplify the variables involved in the analysis, the overloads are not included in the model.

Table 1. Geotechnical parameters.

ID	γ (kN/m3)	c' (kPa)	Φ' (°)	fc (MPa)
Reinforced soil	20.0	0	32°	-
Retained soil	19.0	0	32°	-
Foundation soil	19.0	2	35°	-
Bedrock	22.0	-	-	25.0

Table 2. Parameters of polyester fiber.

	Properties		*UX-60*	*UX-90*	*UX-120*
Physical	Size of the opening - MD ± 20	mm	24	22	21
	Size of the opening - CD ± 20	mm	28	28	28
Mechanical	Stress resistance, T_{ult} - MD min	kN/m	60	90	120
	Elongation - MD	%	10	10	11
	Tensile strength 2% def. - MD min	kN/m	15	23	30
	Tensile strength 5% def. - MD min	kN/m	30	45	60
	Long – Term design tension	kN/m	35	53	71

5. Stability analysis

The design for admissible stress herein presented is based on the concepts and criteria set forth in AASHTO 2002 [4]. With the support of the MSEW v3.0 computer program, the external and internal stability analyses of the reinforced soil wall were performed, optimizing the placement of reinforcements until reaching a final configuration of the structure. Then the global stability analyses for the static and pseudo static conditions, using the SLIDE v6.0 program, were performed. The configuration scheme is presented in Figure 1.

Preliminarily, the configuration of the reinforcement was done for different heights of walls due to the variability of the heights in the longitudinal profile of GSR. The optimization of this configuration was based on the factor of safety. However, only the results of internal and external stability of the GRS wall of 10m height were showed [6].

5.1. External stability

The external stability analysis consists of verifying that the structure does not fail by external mechanisms. That is, do not fail due to sliding at the base, turning due to excessive eccentricity, failure of soil support capacity that can cause a vertical settlement or rotational displacement [6, 7].

The efforts at the base of the reinforced soil block are estimated using the Meyerhof method [8] or the effective area method, while the ultimate capacity is a function of the soil parameters; the relationship between both efforts gives the Factor of Safety (FoS) for bearing capacity.

Table 3 shows the results of the external stability of the GRS for the static and pseudo static conditions. It is observed that the computed safety factors greatly exceed the minimum safety factor value.

Table 3. Security factor under static and seismic conditions.

Item	Condition	
	Static	**Pseudo static**
FoS sliding on the base	2.81 > 1.5	2.16 > 1.5
Ultimate capacity (kPa)	1440.2	1273.9
Effort at the base (kPa)	220.8	249.6
FoS Bearing capacity	6.5 > 2.5	5.1 > 2.5
FoS eccentricity (e/L)	0.0754< 1/6	0.124 < 1/6

5.2. Internal Stability

In the same way, the results of the verification of internal stability are presented the resistance of the reinforcement to traction, resistance to tearing and resistance to sliding between layers [6].

Table 4 and Figure 2 show the safety factors obtained from the analysis of internal stability against the tensile strength of the reinforcing element, the tear strength and eccentricity by layers, and the resistance to sliding between layers for the static and pseudo static conditions.

Table 4. Internal stability.

#	z (m)	kind	Factor of Safety					
			Tensile		Pull out		Sliding	
			(1)	(2)	(1)	(2)	(1)	(2)
15	9.4	I	9.5	5.5	5.6	2.2	33.1	25.4
14	8.4	I	3.6	2.7	6.6	3.6	12.3	9.5
13	7.4	I	2.2	1.8	7.6	4.6	7.5	5.8
12	6.4	I	1.6	1.3	8.7	5.4	5.4	4.1
11	5.4	I	1.7	1.4	13.3	8.0	4.2	3.2
10	4.9	I	2.2	1.7	20.4	11.3	3.7	2.9
9	4.4	I	2.0	1.5	21.4	12.0	3.4	2.6
8	3.9	I	1.8	1.4	22.4	12.7	3.1	2.4
7	3.4	I	1.7	1.3	23.4	13.4	2.9	2.2
6	2.9	I	1.6	1.2	24.4	14.1	2.6	2.0
5	2.4	II	2.2	1.8	25.5	14.8	2.5	1.9
4	1.9	II	2.1	1.7	26.5	15.5	2.3	1.8
3	1.4	II	2.0	1.6	27.5	16.2	2.2	1.6
2	0.9	II	1.9	1.5	28.1	16.7	2.0	1.5
1	0.4	III	1.8	1.5	21.7	13.7	1.9	1.5

Condition: (1) Static (2) Pseudo static.

The values of factors of safety obtained from the verification of the tensile strength that are closest to the minimum are mainly calculated at the base of the wall or when there is a change in stiffness of the reinforcement. In the case of factors of safety obtained from the check for resistance to pullout, they were always lower when closer to the top.

From the results of safety factors in the case of tensile strength, the minimum was given in layer 12, at 6.4 m from the foundation level for the case of static condition.

While in the case of the pseudo static condition, it occurred in layer 6, at a value of 1.2 m to 2.90 m of the base, where a change in stiffness of the reinforcement occurs.

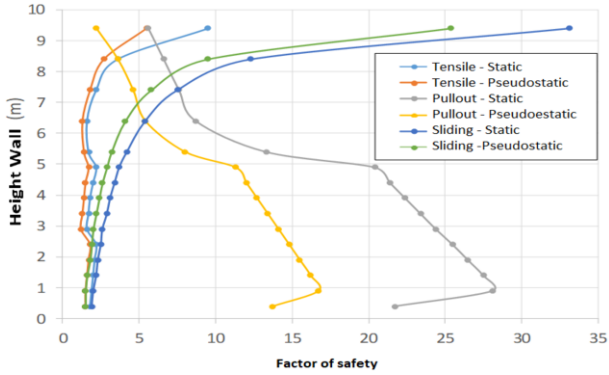

Figure 2. Safety factors derived from internal stability from different height of GRS wall.

The pullout resistance of the reinforcement elements describes the resistance at the interface between reinforcement and soil. If this friction disappears or the relation between stresses is less than one, it is said to have failed by pullout.

For static conditions the minimum value equal to 5.6 was given in layer 15, 9.4 m from the foundation level, while for pseudo static conditions, the minimum value obtained was 2.2 at the same level. It is also observed that when the spacing of 0.5m to 1m between reinforcing elements is increased, the factors of safety are significantly reduced.

Likewise, the factors of safety obtained from the verification of the resistance to sliding between layers will always lower at the base of the wall for both the static and the pseudo static conditions. The minimum value obtained was 1.9 and 1.5, respectively, located 0.4 m from the foundation soil surface.

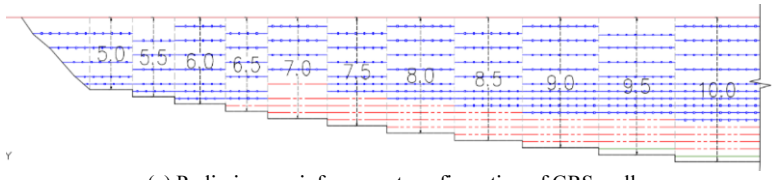

(a) Preliminary reinforcement configuration of GRS wall

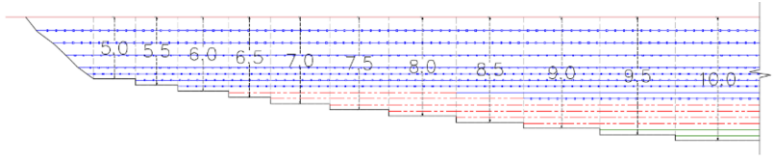

(b) Final reinforcement configuration of GRS wall

Figure 3. Determining the final configuration base in the FoS obtained preliminarily from different height of GRS wall, in order to simulate a real irregular topographic condition.

Figure 2 shows how the factor of safety changes according to the height of the wall, preliminarily internal stability from different height of GRS walls was carried out, this permit to concluded that for this GSR, the critic condition in the tensile resistance of the

reinforcement in the case of the internal analysis under seismic conditions. Moreover, all the preliminary designs were drawn in a longitudinal profile to determine the final reinforcement configuration. Figure 3(a) shows that for a 9.5m height is an important increment in the tensile resistance of the first layer which causes a change in the configuration of the GRS wall at a 10m height shown in Figure 3(b).

5.3. Global stability

The software used for the global stability analysis by the limit equilibrium method was SLIDE v6.0. The minimum factors of safety required in accordance with the regulations were 1.3 in a static condition and 1.1 in a pseudo static condition.

Table 5. Factor of Safety of the Global stability analysis.

Condition	Factor of Safety
Static	1.70
Pseudo static	1.13

Table 5 and Figure 4 present the results of the global stability analysis using the Spencer method of slices, considering a seismic coefficient of 0.19, corresponding to a return period of 475 years.

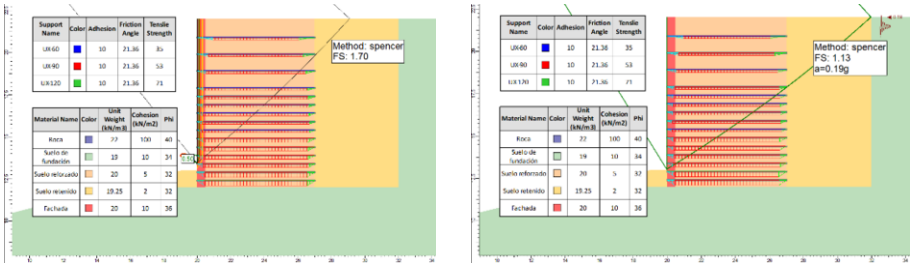

(a) (b)

Figure 4. Global analysis in: (a) static condition and (b) pseudo static condition.

6. Dynamic model

Two-dimensional plane-strain analyses were carried out using FLAC 2D software, based on a Lagrangian calculation scheme that is well suited for modelling large distortions and material collapse. A complete description of the numerical formulation can be obtained in Cundall and Board [9]

Dynamic modeling of earth structures considers the gradual decrease of the shear strength of the soil against a variable dynamic load as a function of time (duration of the seismic event).

The dynamic characterization of geo-materials can be carried out by means of dynamic tests or standard curves of reduction of the shear modulus with cyclic shear strains. With respect to the reinforcement elements, there are studies that have evaluated the cyclic behavior in an isolated manner, while very few investigations have evaluated the complete reinforcement and soil interaction.

Figure 5 shows the finite difference mesh. To avoid loss of accuracy during the wave propagation, the size of the elements was limited to a maximum value given by

Kuhlemeyer and Lysmer [10]. They recommended, as an empirical suggestion, that the size of the element for an efficient transmission of motion does not exceed 1/8 to 1/10 of the lowest expected wavelength in the soil layers:

$$h_{max} = \frac{\lambda_{min}}{10} = \frac{v_s}{10 \cdot f_{max}} \quad (1)$$

where λ_{min} is the wavelength associated with the highest frequency of the input signal fmax and vs is the shear wave velocity. Table 6 shows the values obtained.

Selected sizes were still subjected to the geometry and division between layers of the reinforcement, explaining why the values listed in Table 6 were much lower than the maximum hmax found with Eq. (1).

Table 6. Size elements.

Material	v_s (m/s)	f (Hz)	$h_{máx}$ (m)	$h_{máx}$ (m) selected
structural fill	250 - 500	15	1.6 – 3.3	0.25
foundation soil	450 - 750	15	3 - 5	0.25
rock	750 - 1200	15	5 - 8	0.65

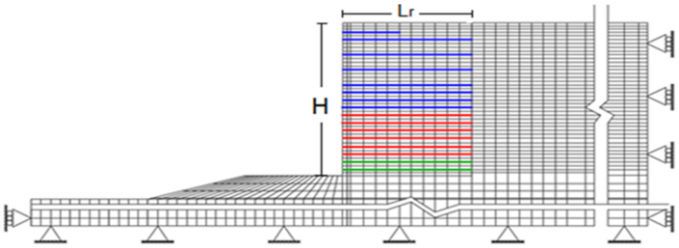

Figure 5. Cross-section of 10m wall in FLAC 2D.

6.1. Soil and geosynthetic

For the dynamic analysis it is necessary to define other parameters see table 7, in addition to those mentioned before (cohesion, friction angle and unit weight), such as elastic modulus and the Poisson's ratio, in order to define the soil constitutive model, in this case the Mohr-Coulomb model.

The hysteretic damping assigned for the foundation soil was adjusted considering the FLAC sig3 model. For the retained and reinforced soils, there is not much information about specific values in the literature, and damping is implicitly associated with the elastoplastic constitutive model. For the rock mass, a Rayleigh damping of 5% was assumed.

Table 7. Soil model parameters.

Parameter	Rock	Foundation	Retained	Reinforced	Facing
E (Pa)	$2.5 \cdot 10^8$	$4.65 \cdot 10^7$	$4 \cdot 10^7$	$5 \cdot 10^7$	$8 \cdot 10^7$
ν	0.22	0.30	0.30	0.35	0.35
γ (kN/m³)	24.04	18.64	19.13	19.62	21.58
ρ (kg/m³)	2450	1900	1950	2000	2200
%	5	*Sig3**		Not specified	
c (kPa)	-	10	2	2	5
φ (°)	-	34	32	32	36

6.2. Reinforcement

In the case of reinforcement, as previously mentioned, uniaxial polyethylene geogrids of high strength were chosen. As indicated in the FLAC manual, the geosynthetic reinforcement layers can be represented as either cable, beam or strip elements. Similar studies suggest that assigning the cable type element has correctly simulated the behavior of uniaxial geogrid.

Figure 6 shows the initial stiffness, the 2% and the 5% stiffness of deformation of the reinforcement proposed by Cai and Bathurst [11] to determine the secant stiffness. In addition, if the stiffness value is multiplied by the coverage ratio of each element between the area of the reinforcement, it gives the modulus of elasticity of the reinforcement, according to the proposal suggested by Yu et at. [12].

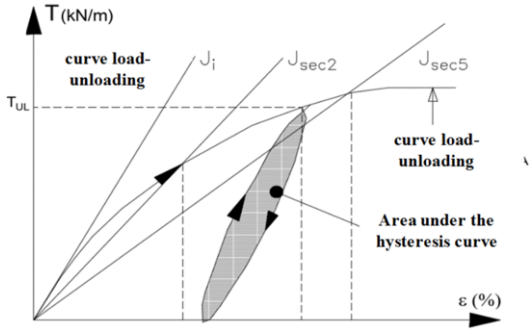

Figure 6. Curve obtained from loading-unloading tests in a uniaxial geogrid [11].

$$E_r = J_{\mathrm{sec}(\varepsilon\%)} * \frac{R_c}{A_{xr}} \tag{1}$$

See Eq. (2), where E_r is modulus of elasticity of the reinforcement, $J_{\mathrm{sec}}(\varepsilon\%)$ is the secant stiffness at ε % of strain, R_c is coverage ratio ($R_c = A_{xr}$ / thickness) and A_{xr} is the section area of the reinforcement element.

Table 8 summarizes the parameters that defines the mechanical behavior of the reinforcement in the dynamic analyses.

Table 8. Properties of reinforcement geogrid.

Description	Test ASTM	Uniaxial grid		
		UX60	UX90	UX120
Average stiffness	kN/m/m	1100	1675	2200
Initial stiffness $J_{2\%}$	kN/m/m	1000	1545	2000
Initial stiffness $J_{5\%}$	kN/m/m	1200	1800	2400
Elasticity module	N/m^2	$1.76 \cdot 10^8$	$2.64 \cdot 10^8$	$3.52 \cdot 10^8$

6.3. Soil-reinforcement interface

Defining the geogrid as a cable reinforcement element allows resistance values to be entered between reinforcement and soil, due to the contact of the lateral area of the reinforcement with the soil. The values of shear stiffness and normal stiffness to tearing were taken from the literature, just as it is also feasible to define a friction angle of the

interface. Rowe and Skinner [13] recommended that in the case of interfaces to take 80% of the friction angle of the weakest material.

The characterization of the reinforcement to perform the numerical modeling was based on a pullout test between a granular soil with ϕ= 35°, γ = 19kN/m^3 and uniaxial geogrid reinforcement T_{UL} = 125kN/m. Table 9 presents the values defined for the interface by other authors and in the present study.

Table 9. Properties of reinforcement geogrid.

Reference	K_s Shear stress (kN/m/m)	K_n Axial stiffness (N/m)	ϕ (°)	c (kPa)
Cai and Bathurst [11]	9600	1000	35°	-
Rowe and Skinner [13]	-	-	29°	-
Skinner and Rowe [14]	-	-	31.5°	-
Huang, Bathurst et al. [15]	1000	1000	44°	-
C. Torres [6]	10000	1000	26°	10

6.4. Input ground motions

The advantage of using FLAC in seismic analysis is the simplicity of applying seismic loading at the bottom boundary of the mesh, i.e. at the bedrock level, through input accelerograms, such as the one shown in Figure 7.

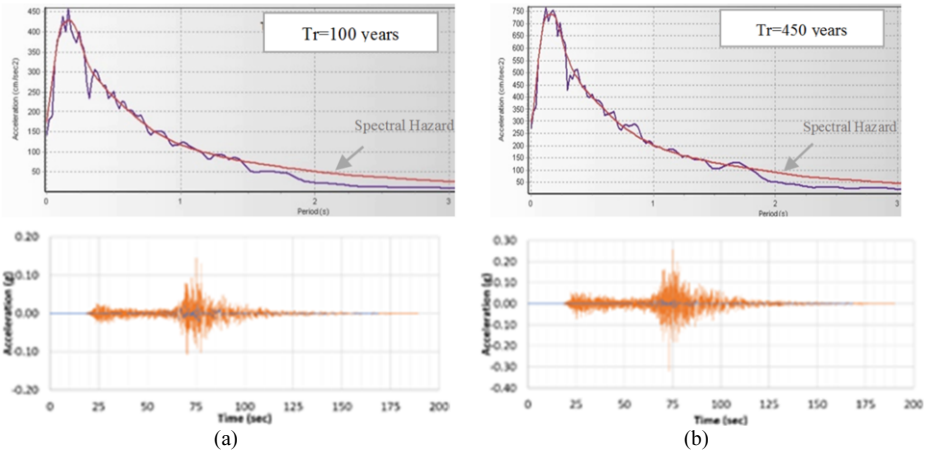

(a) (b)

Figure 7. Matching and synthetic accelerometer for a time of return of a) Tr = 100 years; b) Tr = 475 years.

6.5. Dynamic analysis

To continue with dynamic analysis in FLAC 2D, the dynamic option is activated, and the mechanical calculation is assigned for large deformations. In some cases, it is important to update the grid of the model during execution (rezoning) to prevent the execution stopping in the middle of the analysis. For the present study, it was verified, in a preliminary analysis, that a zone of excessive deformation could cause the interruption of the analysis, and a reinforcement element was included to avoid this occurrence at the foot of the wall. In engineering practice this corresponds to an improvement of the first layers of the foundation soil.

6.5.1. Displacement fields

The computed permanent horizontal displacements are less than 35cm and 75cm on the crest of the GRS wall, 20cm and 35cm at the base of the wall, for earthquakes of 100 and 475 years of return period, respectively. The relative horizontal displacement of the facade of the reinforced soil wall with respect to the base was 15 cm and 40 cm, respectively. According to Figures 8 and 9, these values correspond to 1.5 and 3% of the total height of the wall for each return period.

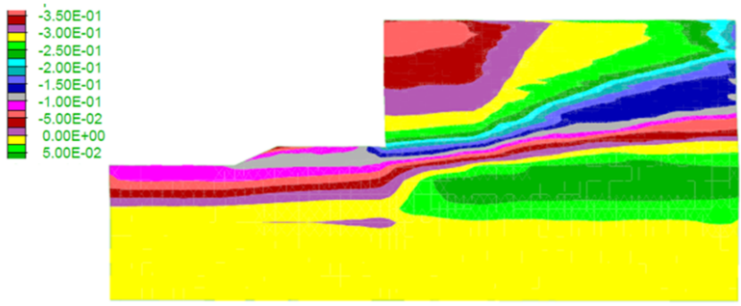

Figure 8. Contours of horizontal displacement at end of analysis with Tr = 100 years.

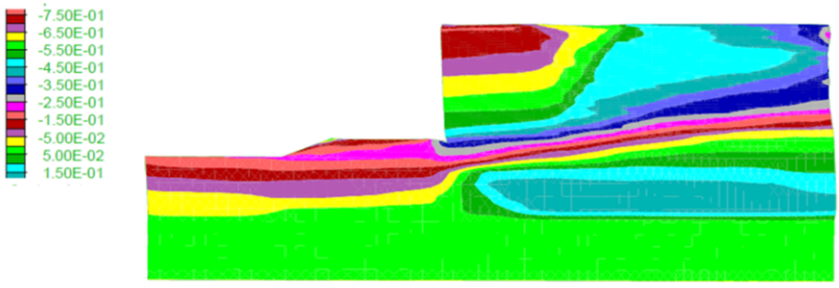

Figure 9. Contours of horizontal displacement at end of analysis with Tr = 475 years.

Likewise, it is observed that the wall has a slight forward movement, which causes a decrease in stress in the rear part of the reinforced soil block. It is important to note that the most critical area in a dynamic analysis in a GRS wall. They are strains that occur at the base of the wall, since these are the ones that will cause the wall to tend to fail by turning.

On the other hand, Figure 10 shows the permanent vertical displacements obtained for the dynamic analyses subjected to synthetic earthquakes with return periods of 100 and 475 years. These values are 7.5cm and 25cm, respectively. The maximum displacements are displayed behind the reinforced soil zone, reaching values of 12.5 cm and 30.5 cm respectively (settlement of the platform of GRS wall).

6.5.2. Relative displacements

FLAC 2D software, through the FISH programming language, allows defining additional variables. This is how the calculation of relative displacements between layers or vertical points is implemented. The node of the mesh in which the geogrids will be fixed is

identified, considering the first layer as (i, j_{c1}), the second as (i, j_{c2}), and so on. Equation 3 computes the relative displacements as shown in Figure 10.

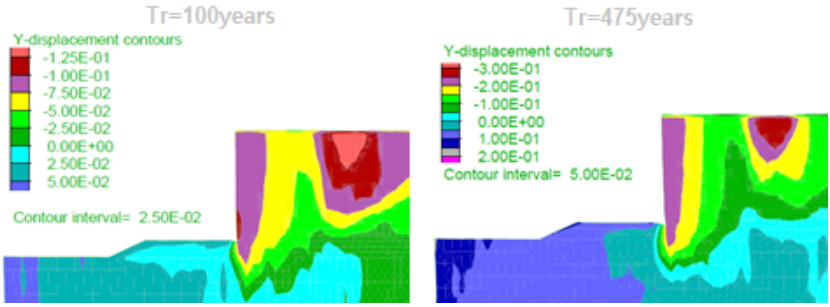

Figure 10. Contours of vertical displacements.

$$X_{rel1}=X_{DISP}(i,j_{c2}) - X_{DISP}(i,j_{c1}) \quad (3)$$

Figure 11 shows the configuration of relative displacement variables and Figure 12 shows the relative displacements due to seismic events with return period of 100 years (maximum of 3.5 cm between the reinforcement layers) and 475 years (maximum value of 8 cm).

Figure 11. Configuration of relative displacement variables.

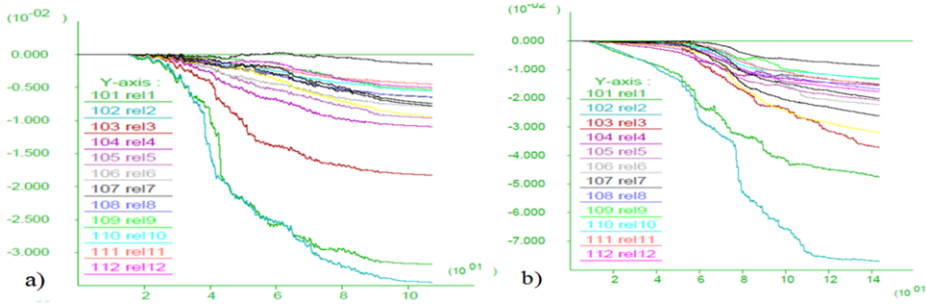

Figure 12. Relative displacements between layers on the front of the GRS wall to a) T_r = 100; b) 475 years.

The maximum axial forces in the reinforcement elements were all below the value of maximum admitted tension, as can be seen in Figure 13. In the case of layer 1 (0.4 m from the base), the axial force was lower than 50 kN, which is less than 50% of the ultimate tension stress supported by the reinforcement (120 kN). In layer 3 (1.4 m from the base) and in layer 13 (6.9 m from the base) the corresponding values were less than 30 kN and 28 kN, namely 35% and 50% lower than the ultimate tension stress of 90 kN and 60 kN, respectively. From the computed values, it is observed that the wall of reinforced soil will not fail due to sliding of the face of the wall.

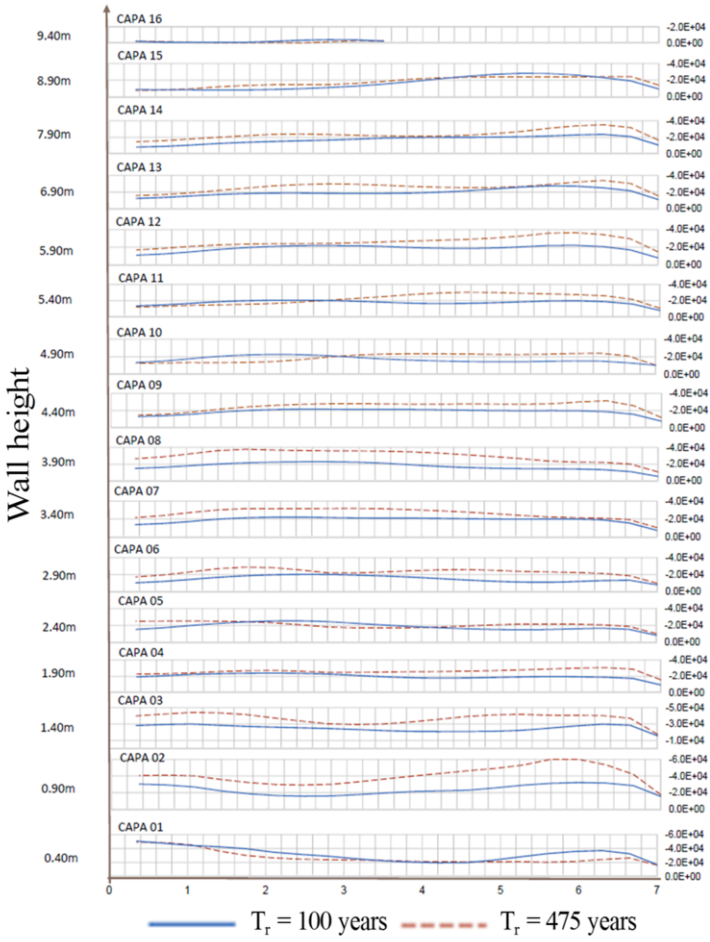

Figure 13. Axial forces (N) along each reinforcement at the end of the analysis for a synthetic earthquake with return periods of 100 and 475 years.

In the present study, the reinforcements were denominated as cable 1, cable 2, and so on up to cable 16, located at 0.4, 0.9, and so on up to 9.4 times the height of the GRS wall. Then, it was identified at what distance from the reinforcement the maximum tension occurred, the points were connected, and the possible failure surface was obtained for dynamic analyses, as shown in Figure 14, for dynamic analyses considering earthquakes with 100 and 475 return periods.

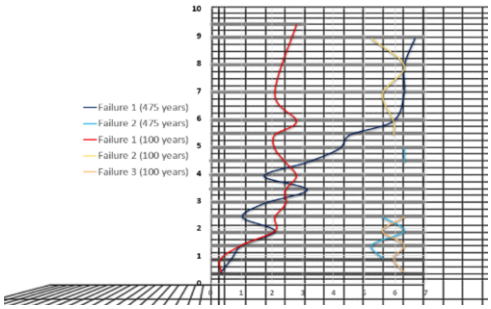

Figure 14. Location of possible failure surfaces linking points of maximum axial forces in the geogrids.

7. Conclusions

The GRS walls are designed following international standards. In Peru, there are only a few recommendations for these structures within the Manual of the Ministry of Transport and Communications (MTC).

Doing a preliminary analysis for walls of different heights show the importance of designing the reinforcement configuration for the maximum height (h_{max}) in the GSR, the $h_{max\text{-}0.5m}$ and $h_{max\text{-}1m}$, in order to guarantee the continuity of the reinforcement and the stability along the longitudinal profile.

The practice of increasing the length of the reinforcement, from 0.7 to 0.8 times the height of the wall, when it is designed for a highly seismic zone, has no technical justification, raising the costs of the geotechnical structure. For our study a reinforcement length equal to 0.7 times the height was considered, obtaining satisfactory results.

The limit equilibrium method used for pseudo static analyses can be excessively conservative and does not provide information on deformations; therefore, numerical analysis is justified in cases of high-risk seismic events. The factors of safety, either for the static condition with a minimum value of 1.3 or for the pseudo static analysis with 1.1, have complied to the standard and it is possible to state that the GRS wall is stable.

Pamuk et al. [2] and E-Emma et al. [16], when comparing deformations between numerical and physical models, found that the GSW behaves mainly as a block due to the soil-reinforcement effects. The block type behavior was also confirmed during the present dynamic analysis, with the block having the tendency to make a slight forward movement, which causes a decrease in stresses in the rear part of the reinforced block base. Hence, it is possible to conclude that the most critical area in a dynamic analysis of a GSW is in the foundation soil at the base of the wall, where the occurrence of excessive deformations (horizontal or vertical) may cause the failure of the GSW by flipping. Although in a GSW design the reinforcement behavior is main concern (slip failure, rupture or tearing), this did not occur in any of the cases analyzed in the present research.

In this work, it was also observed that the transmission of loads between reinforcement layers actually occurred, which allowed a reduction of the lateral stresses under static condition that affected the computed displacements, a similar result reported by Rowe and Skinner [13]

The maximum stresses in the reinforcement elements reached 50% of ultimate value for the UX-90 and UX-12 geogrids and 70% in the case of UX-60 geogrid.

Finally, it may be concluded that the most important factors in the reduction of permanent deformations in a GSW wall subjected to seismic loading are the length and shear strength of the reinforcement and the movement in the base of the wall. If these three factors are carefully considered, failure by turning of the reinforced block may be prevented.

References

[1] Burke, C., Ling H.I. Y Liu H. (2004) "Seismic response analysis of a full-scale reinforced soil retaining wall", 17th ASCE Engineering mechanics conference, Delaware, USA.

[2] Pamuk, A.; Ling, H.I.; Leshchinsky, D.; Kalkan, E.; Adalier, K. (2004). "Behavior of reinforced wall system during the 1999 Kocaelli (Izmit), Turkey, Earthquake", *5th Intenational conference on case histories in geotechnical engineering*, New York, USA, Paper N° 3.45.

[3] Koerner, R. M. (2012). "Designing with geosynthetics", 6th edition Vol 1, Xlibris Corporation, USA.

[4] Federal Highway Administration - FHWA (2000). Mechanically stabilized earth walls and reinforced soil slopes design & construction guidelines - FHWA-NHI-00-043. Washington, D.C.

[5] Federal Highway Administration - FHWA (2011). Seismic analysis and design of transportation geotechnical features and structural foundations - FHWA-NHI-11-032. Washington, D.C.

[6] Torres, C (2018) "Evaluación de comportamiento sísmico de muros de suelo reforzado con geomallas por métodos numéricos" Thesis to obtain the title of Civil Engineer in Engineering National University, Lima-Peru.

[7] Torres, C.; López M.; Zegarra J.; Romanel C. (2018); "Seismic analysis of a geosynthetic-reinforced soil retaining wall in Peru" XIX Congresso Brasileiro de Mecânica dos Solos e Engenharia Geotécnica COBRAMSEG 2018

[8] Meyerhof, G.G. (1951). "The ultimate bearing capacity of foundations". *Géotechnique*, Vol. 2, Issue 4, p. 301-332.

[9] Cundall, P.; Board, M. (1988). "A microcomputer program for modelling large-strain plasticity problems", *Proceedings of the 6th International Conference on Numerical Methods in Geomechanics*. Innsbruck, Austria, p. 2101-2108.

[10] Kuhlemeyer, R.L. and Lysmer. J. (1973) "Finite Element Method Accuracy for Wave Propagation Problems", *Journal of the Soil Dynamics Division*, 99, p. 421-427.

[11] Cai, Z.; Bathurst, R.J. (1995). "Seismic response analysis of geosynthetic reinforced soil segmental retaining walls by finite element method", *Computers and Geotechnics* 17, Elsevier, UK, p. 526-546.

[12] Yu, Y.; Bathurst R.J.; Allen T.M. (2016). "Numerical modeling of the SR-18 geogrid reinforced modular block retaining walls", *Journal of Geotechnical and Geoenvironmental Engineering*, ASCE, ISSN 1090-0241.

[13] Rowe, R.K.; Skinner, G.D. (2001). "Numerical analysis of geosynthetic reinforced retaining wall constructed on a layered soil foundation", *Geotextiles and Geomembranes 19*, Elsevier, p. 387-412.

[14] Skinner G.D. Y Rowe R.K., (2005) "Design and behavior of a geosynthetic reinforced retaining wall and bridge abutment on a yielding foundation" Geotextiles and Geomembranes 23.

[15] Huang, B. Bathurst, R. Y Hatami, K., (2009) "Numerical study of reinforced soil segmental walls using three different constitutive soil models". Journal of geotechnical and geoenvironmental engineering, ASCE.

[16] El-Emam, M.M.; Bathurst, R.J; Hatami, K. (2004). "Numerical modeling of reinforced soil retaining walls subjected to base acceleration", *13th World conference on earthquake engineering*. Vancouver, B.C., Canada, 13WCEE, N° 2621.